

# Many-Body Vertex Effects: Time-Dependent Interaction Kernel with Correlated Multi-Excitons in the Bethe-Salpeter Equation

Brian Cunningham<sup>1</sup>

<sup>1</sup>*NI-HPC, Queen's University Belfast, Belfast BT7 1NN, Northern Ireland, United Kingdom*

Building on a beyond-*GW* many-body framework that incorporates higher-order vertex effects in the self-energy —giving rise to *T*-matrix and second-order exchange contributions —this approach is extended to the kernel in the Bethe-Salpeter Equation (BSE) for the reducible polarization. This results in a frequency-dependent interaction kernel that naturally captures random phase approximation (RPA) effects, dynamical excitonic interactions, and the correlated propagation of multiple correlated electron-hole pairs that model multi- (including bi- and tri-) excitonic effects, relevant for nonlinear optics and high harmonic generation. These processes emerge from including the functional derivatives of the screening and vertex with respect to the Green's function in the vertex, enabling a fully *abinitio*, time-dependent treatment of correlation effects. By focusing on the reducible rather than irreducible polarization, this approach provides a computationally viable framework for capturing complex many-body interactions for calculating the self-energy, optical spectra and EELS. The resulting interaction kernel is relatively straightforward and clearly delineates the physical processes that are included and omitted. The method is expected to facilitate the integration of advanced many-body effects into state-of-the-art software packages, offering a universal and highly accurate framework for the description of sub-atomic correlations. Such advancements are crucial for the development of semiconductor, optoelectronic, superconducting and antimatter technologies, and ensuring that theoretical modeling evolves alongside exascale and accelerated computing.

PACS numbers: 42.25.Bs, 11.10.St, 71.15.-m, 78.20.-e

## I. INTRODUCTION

Advancing our understanding of sub-atomic particle interactions — such as electron-electron, electron-nucleus, and electron-positron interactions — is essential for increasing our understanding of the universe, and driving progress in technology, medicine and computation. The Kohn-Sham formulation of density functional theory (DFT)[1, 2] is the most widely used method for studying electronic interactions due to its balance of accuracy and efficiency. DFT continues to evolve, being applied to real-world problems, however, despite the success of DFT and its extensions, such as generalized Kohn-Sham schemes[3], DFT+U,[4] and DFT+DMFT,[5] its limitations in strongly correlated systems necessitate the development of more accurate many-body approaches

Whilst it is important we continue to further refine and extend DFT-based methods, it is equally important to develop higher-accuracy approaches, such as wavefunction methods[6] and many-body theory.[7] DFT struggles when applied to strongly correlated systems such as NiO.[8–10] Recent rapid advances in exascale and GPU computing[6, 11] suggest that computationally expensive methods — approaching current practical limits — may become viable in the near future. Wavefunction methods, while highly accurate, are often restricted to the calculation of ground-state properties in smaller systems, requiring significant effort to extract additional information that quite often is not of any use[12].

To address these challenges, many-body theory (MBT) approaches, particularly those based on Lars Hedin’s formalism,[7] provide a promising balance between accuracy and computational efficiency. A real benefit of the approach is that it is *ab initio* and can be extended with the addition of more diagrams describing processes missing from a particular implementation[13]. MBT also has the benefit that excited state phenomena (required for investigating, e.g., optoelectronic phenomena) are readily computed. Most MBT implementations are based on the  $GW$  approximation[14–16] to Hedin’s equations. Whilst an improvement over DFT, many implementations are simply a first-order perturbation applied to the DFT electronic structure, and as a result depend on the choice of DFT functional chosen, and therefore tend to perform poorly in strongly correlated systems.[17, 18] Another key issue with  $GW$  is the inadvertent cancellation of errors due to missing diagrams, which can lead to seemingly accurate results for specific quantities, such as band gaps, while failing to capture other important physical phenomena, and quantities such as the total energy.[19, 20] Although this may prove beneficial in certain circumstances, its important we do not overlook this, as certain physical processes may not be captured at all, limiting the method’s predictive reliability in unexplored materials. Self-consistent approaches remove the starting-point dependence by iterating the  $GW$  formalism, however, these can also prove problematic.[8, 21] The quasiparticle self-consistent  $GW$  (QS $GW$ ) method[9, 18, 22, 23] is one such method that has become popular in recent years. However, conventional QS $GW$  ignores vertex effects in both the polarization and self-energy and as a result performs worse in simple systems due to one of the competing effects now being included and no longer cancelling with another missing effect.

To address these shortcomings, researchers have explored incorporating vertex effects in the polarization and/or self-energy. Inclusion of vertex effects in the polarization through solving the Bethe-Salpeter equation (BSE) has become popular in recent years[24–26]. Solving the BSE with an effective non-local static kernel derived from time-dependent DFT[27–29] has become a common approach. Another approach is to solve the BSE with the kernel  $i\delta\Sigma/\delta G$  (the functional derivative of the self-energy with respect to the Green’s function) calculated with the  $GW$  approximation for  $\Sigma$ , whilst neglecting  $\delta W/\delta G$  and assuming a static kernel. We used the latter for the QS $\widetilde{GW}$  method in the Questaal code[9, 30] to capture excitonic effects in strongly correlated systems such as NiO for optical spectra and to also improve the electronic structure. In those works we calculated  $W$  at the level of the random phase approximation (RPA). Whilst an improvement on QS $GW$  there are still many effects missing from the method, such as time-dependent interactions in the BSE and multiexcitonic effects. Time-dependence in the interaction kernel is examined in Ref. [31, 32] and shown to strongly affect optical spectra in noble metals.[31] Multiexcitonic effects[33, 34] describe the process of a number of interacting electron-hole pairs propagating in the system. These effects are crucial for examining optoelectronic phenomena such as high-harmonic generation[35] and non-linear effects.

Another effect missing in the QS $\widetilde{GW}$  method is the vertex in the expression for the self-energy. Methods exist for including vertex effects in the self-energy, such as those developed by Kutepov[36, 37], showing the significance of these effects in predicting flat, dispersionless bands in materials like the copper halides CuCl and CuBr.[9, 38] The multichannel Dyson equation method[39] and the method outlined in Ref. [40] also included vertex effects in the self-energy. Recently, the author developed a method for including vertex effects in the self-energy,[13] yielding a relatively straightforward expression for the self-energy, that extends  $GW$  by incorporating  $T$ -matrix diagrams and the second-order statically screened exchange. In that work the benefit of working with the reducible polarization instead of the irreducible one was made clear. We also examined a similar method with the inclusion of the  $T$ -matrix diagrams applied to the case of a positron interacting in finite systems,[41] with the additions proving essential for capturing positron physics (describing processes such as virtual positronium formation) and accurately predicting positron binding energies[41] and scattering and annihilation rates.[42]

In this work, the beyond- $GW$  formalism introduced in Ref. [13], that derives an analytic expression for the interaction kernel  $i\delta\Sigma/\delta G$  from Hedin’s equations, is extended to examine these effects in the polarization. The approach incorporates time-dependent effects and multiexcitonic interactions, addressing key limitations of conventional BSE formulations. By including the functional derivative of the vertex from  $\Sigma = iGWT$ , correlations between separate electron-hole pairs, including higher-order exchange effects, arise. These new additions give rise to effects beyond the standard BSE, including multiexcitonic effects.

The derivation is performed in the time domain before being transformed to frequency, and the key steps are presented for the possibility of examining, e.g., time-dependent interactions in the  $T$ -matrix diagrams in the future. The method relies on using the reducible polarization  $\Pi$  instead of the irreducible one, as the screening is simply  $v + v\Pi v$ , instead of  $(1 - vP)^{-1}v$  for the irreducible one. The final expression is depicted with diagrams illustrating the processes included in the formalism. The result is a matrix equation for the reducible polarization akin to the usual BSE, but now with a frequency dependent interaction kernel that contains higher order diagrams. The suppression of self-polarization effects (more pronounced in strongly correlated systems) emerges naturally in this framework. The approach is general, intuitive and does not rely on empirical or ad-hoc parameters/interactions and is fully self-contained, having the potential to be implemented in various many-body electronic structure and even antimatter[41] software packages.

## II. DERIVATION OF THE POLARIZATION

The single particle Green's function in the frequency domain is

$$G(\mathbf{r}, \mathbf{r}', \omega) = \sum_n \frac{\varphi(\mathbf{r})\varphi^*(\mathbf{r}')}{\omega - \varepsilon_n \pm i\eta}, \quad (1)$$

where  $\varphi_n$  and  $\varepsilon_n$  are the eigenfunctions and eigenvalues of the corresponding Hamiltonian and the  $+(-)$  is for particles(holes).  $n$  may be a composite index subsuming spin and orbital index, or band index and  $\mathbf{k}$  in extended systems. The inverse Fourier transform  $\frac{1}{2\pi} \int G(\mathbf{r}, \mathbf{r}', \omega)e^{-i\omega t} d\omega$ , produces

$$G(\mathbf{r}, \mathbf{r}', t) = \mp i \sum_n \varphi(\mathbf{r})\varphi^*(\mathbf{r}')e^{-i\varepsilon_n t} e^{\mp\eta t} \theta(\pm t), \quad (2)$$

where the transformation is calculated using the Cauchy residue theorem,  $\pm 2\pi i \sum_{\text{residues}}$ , with the contour taken in the upper plane for  $t < 0$  (holes) and in the lower plane for  $t > 0$  (particles) to ensure convergence of  $e^{\mp\eta t}$  as  $|t| \rightarrow \infty$ . This will be useful for determining the interaction kernel later. The Green's function is diagonal in the basis of the single particle states  $\varphi_n(\mathbf{r})$ . From the Hedin equation for the irreducible polarization[7, 13, 43]  $P(1, 2) = -iG(1, 3)G(4, 1)\Gamma(3, 4; 2)$  (with  $1 = (\mathbf{r}_1, t_1, \sigma_1)$  and repeated indices on one side of the equality implying summation/integration) the zeroth order term without the vertex in the basis of particle-hole states (refer to Eq. (19) in Ref. [13]) is

$$P_{n_3 n_4}^{n_1 n_2}(\omega) = \frac{f_{n_2} - f_{n_1}}{\omega - \varepsilon_{n_1} + \varepsilon_{n_2} + (f_{n_2} - f_{n_1})i\eta} \delta_{n_1, n_3} \delta_{n_2, n_4} \quad (3)$$

with  $f$  the single particle occupations, 0(1) for a particle(hole), also denoted  $c(v)$  for conduction(valence). In the time domain this is

$$P_{n_3 n_4}^{n_1 n_2}(t) = -ie^{-i(\varepsilon_{n_1} - \varepsilon_{n_2})t} e^{\mp\eta t} \theta(\pm t) \delta_{n_1, n_3} \delta_{n_2, n_4}, \quad (4)$$

where the upper(lower) sign is for  $n_1, n_2$  a particle-hole(hole-particle) pair. This represents the forward propagating non-correlated electron-hole propagator (or backward travelling hole-particle propagator). Let's now take Hedin's equations for the polarization and many-body vertex,[7, 43]

$$\Gamma(1, 2; 3) = \delta(1, 2)\delta(2, 3) + \frac{\delta\Sigma(1, 2)}{\delta G(4, 5)} G(4, 6)G(7, 5)\Gamma(6, 7; 2), \quad (5)$$

with  $\Sigma$  the self-energy. As discussed in Ref. [13] the reducible polarization  $\Pi = P + Pv\Pi$ , where  $v(\mathbf{r}, \mathbf{r}') = 1/|\mathbf{r} - \mathbf{r}'|$  is the bare Coulomb potential, can replace the irreducible one, with

$$\Pi(1, 2) = P^0(1, 2) + P^0(1; 3, 4)K(3, 4; 5, 6)\Pi(5, 6; 2), \quad (6)$$

and the 3-point extensions of the polarization are used<sup>1</sup> and  $K(3, 4; 5, 6) = v(3, 5)\delta(3, 4)\delta(5, 6) + i\delta\Sigma(3, 4)/\delta G(5, 6)$ .

The functional derivative of the self-energy is presented in Ref. [13] and when considered explicitly in the self-energy,  $\Sigma(1, 2) = iG(1, 3)W(4, 1)\Gamma(3, 2; 4)$  (with  $W = v + v\Pi v$  the screened interaction), gives rise to higher-order diagrams that

<sup>1</sup> The four-point  $P^0(1, 2; 3, 4) = -iG(1, 3)G(4, 2)$  is obtained by 'opening the legs' of the two-point polarization.

include the second-order screened exchange and diagrams describing the infinite series of 2-body ladder interactions between the added particles (or holes as the result of particle removal) and the excited electrons or holes in the system. These diagrams will now be included in the expression for the reducible polarization. To do so, an expression for  $\Pi$  with a time-dependent interaction kernel will need to be derived. If only the first term in Eq. (14) for  $i\delta\Sigma/\delta G$  from Ref. [13] is taken (i.e., adopting the  $GW$  approximation for  $\Sigma$  and ignoring  $\delta W/\delta G$ ) and also assumed static (the  $\omega = 0$  contribution) then the usual static Bethe Salpeter Equation (BSE)[9, 24, 25, 44] can be derived from Eq. 6. The screening in the basis of particle-hole pairs is then

$$W_{\substack{n_1n_2 \\ n_3n_4}}(\omega) = V_{\substack{n_1n_2 \\ n_3n_4}} + \sum_{\substack{n_5n_6 \\ n_7n_8}} V_{\substack{n_1n_2 \\ n_5n_6}} \Pi_{\substack{n_5n_6 \\ n_7n_8}}(\omega) V_{\substack{n_7n_8 \\ n_3n_4}}, \quad (7)$$

and for the simple vertex  $i\delta\Sigma(3, 4)/\delta G(5, 6) = -W(4, 3)\delta(3, 5)\delta(4, 6)\delta(t_3 - t_4)$ ,

$$\Pi_{\substack{n_1n_2 \\ n_3n_4}}(\omega) = (f_{n_4} - f_{n_3}) \sum_{\lambda} \frac{X_{n_1n_2, \lambda} X_{\lambda, n_3n_4}^{-1}}{\omega - E_{\lambda} + i(f_{n_4} - f_{n_3})\eta}, \quad (8)$$

where  $X$  and  $E$  are the eigenvectors and eigenvalues of the 2-particle matrix  $H_{\substack{n_1n_2 \\ n_3n_4}} = (\varepsilon_{n_1} - \varepsilon_{n_2})\delta_{n_1n_3}\delta_{n_2n_4} \pm K_{\substack{n_1n_2 \\ n_3n_4}}$ , with  $+$ ( $-$ ) for  $n_1$  a particle(hole). In this case,  $K_{\substack{n_1n_2 \\ n_3n_4}} = V_{\substack{n_1n_2 \\ n_3n_4}} - W_{\substack{n_4n_2 \\ n_3n_1}}(\omega = 0)$ . Calculating the BSE for the reducible polarization has the benefit of being able to calculate the poles of  $W$  (exactly equal to the poles of  $\Pi$ ) and to determine the  $GW$  self-energy, we no longer need to construct and invert the dielectric matrix and perform numerical frequency integration (as in Ref. [18]), nor is, e.g., the plasmon-pole approximation required. Another benefit of calculating  $\Pi$  is that it is of the same structure as  $P^0$  above and can be written in the time domain as the sum of a static part and terms describing forward or backward propagation and so the screening is then

$$W(t) = V\delta(t^+) + W^+(t)e^{-\eta t}\theta(t) + W^-(t)e^{+\eta t}\theta(-t), \quad (9)$$

where  $t^+ = t + \eta$  and

$$W_{\substack{n_1n_2 \\ n_3n_4}}^{\pm}(t) = -i \sum_{\substack{\lambda \\ n_5n_6}} V_{\substack{n_1n_2 \\ n_5n_6}} X_{n_5n_6, \lambda} X_{\lambda, ph(hp)}^{-1} e^{-iE_{\lambda}t} V_{\substack{ph(hp) \\ n_3n_4}}, \quad (10)$$

where the upper(lower) sign corresponds to  $t > (<)0$  and the summation is restricted to particle-hole(hole-particle) pairs depending on the sign of  $t$ . Note that to reduce memory requirements  $VX$  can be calculated (or rather its two contributions) and transformed to an auxillary or reduced mixed product basis, as in Ref. [18, 45].

To include higher order terms in the kernel (as in Ref. [13]), a time-dependent interaction kernel is required. This also allows the incorporation of dynamical excitonic effects, as discussed in, e.g., Ref. [31, 32]. To do so, let's take Eq. 6 and assume  $t_3 = t_4$  and  $t_5 = t_6$  (i.e., the kernel is only dependent on a single time difference) and Fourier transform the expression from the time domain, with the four-point  $P^0$  expressed in terms of the Green's functions. Begin by determining the first term in the expansion,  $\Pi = P^0 + P^0 K P^0 + \dots$ , which can be extended to higher-order terms, whilst focusing only on the dynamical parts of the interactions for now,

$$\Pi_{\substack{n_1n_2 \\ n_3n_4}}^1(\omega) = (-i)^2 \int \int dt dt_3 dt_4 e^{i\omega t} G_{n_1}(t_1 - t_3) G_{n_2}(t_4 - t_1) K_{\substack{n_1n_2 \\ n_3n_4}}(t_3 - t_4) G_{n_3}(t_3 - t_2) G_{n_4}(t_2 - t_4), \quad (11)$$

with  $t = t_1 - t_2$ .  $n_1n_2$  and  $n_3n_4$  will be particle-hole or hole-particle, but will be the same when the Tamm-Dancoff approximation[46, 47] (TDA) is adopted. To solve, use the expression for the Heaviside step function  $\theta(t) = \lim_{\eta \rightarrow 0^+} 1/2\pi i \int e^{ixt}/(x - i\eta) dx$  and make use of the relation  $\int e^{i\omega t} dt = 2\pi\delta(\omega)$ , whilst making sure the contour is placed in the correct plane to ensure the poles are such that terms  $e^{ixt}$  do not diverge for complex  $x$  as  $|t| \rightarrow \infty$ . For  $n_1n_2$  and  $n_3n_4$  both particle-hole pairs,

$$\Pi_{\substack{n_1n_2 \\ n_3n_4}}^1(\omega) = \frac{i}{\varepsilon_{n_1} - \varepsilon_{n_2} - \omega - i\eta} \int_0^{\infty} dt_3 \int_0^{t_3} dt_4 \left\{ \begin{aligned} & K_{\substack{n_1n_2 \\ n_3n_4}}(t_3 - t_4) e^{i(\varepsilon_{n_2} - \varepsilon_{n_3} + \omega + i\eta)t_3} e^{i(\varepsilon_{n_4} - \varepsilon_{n_2} - i\eta)t_4} + \\ & K_{\substack{n_1n_2 \\ n_3n_4}}(t_4 - t_3) e^{i(\varepsilon_{n_4} - \varepsilon_{n_1} + \omega + i\eta)t_3} e^{i(\varepsilon_{n_1} - \varepsilon_{n_3} - i\eta)t_4} \end{aligned} \right\} \quad (12)$$

where the terms arise from the two possible time orderings of the interaction. Upon changing the integration variable  $t = t_3 - t_4$  we get  $\int_0^\infty dt_3 \int_0^{t_3} dt$  for the first term, that can be reordered as  $\int_0^\infty dt \int_t^\infty dt_3$ , and upon reintroducing the step function one obtains

$$\Pi^1(\omega) = P_{n_1 n_2}^0(\omega) \tilde{K}_{n_1 n_2, n_3 n_4}(\omega) P_{n_3 n_4}^0(\omega), \quad (13)$$

with

$$\tilde{K}_{n_1 n_2, n_3 n_4}(\omega) = \int_0^\infty dt e^{\pm i(\omega + \varepsilon_{n_2} - \varepsilon_{n_3})t} K_{n_1 n_2, n_3 n_4}(\pm t) + \int_0^\infty dt e^{\pm i(\omega + \varepsilon_{n_4} - \varepsilon_{n_1})t} K_{n_1 n_2, n_3 n_4}(\mp t), \quad (14)$$

where the upper(lower) sign is for  $n_1 n_2, n_3 n_4 = ph, ph(hp, hp)$ . Comparing to the work of Marini and Del Sole[31], the kernel has two terms, corresponding to the two time orderings of the interaction and is expressed as the Laplace transform ( $\int_0^\infty e^{-st} f(t) dt$ ) calculated at  $\mp i(\omega + \varepsilon_{n_2} - \varepsilon_{n_3})$  and  $\mp i(\omega + \varepsilon_{n_4} - \varepsilon_{n_1})$ , and for direct comparison replace  $n_1 n_2, n_3 n_4$  with  $v_1 c_1, v_2 c_2$  or  $c_1 v_1, c_2 v_2$ . It is also important to note that for the time reversed part of the interaction, integrating for positive times requires calculating the Laplace transform of  $K(-t)$  as this contribution is zero for  $t > 0$ . The kernel can be written as a combination of an instantaneous and a forward and backward propagating interaction, as shown for the screening above and will be discussed below for the other terms that appear in the expression for the vertex. Focusing only on the screening in the vertex for now (the term that gives rise to the usual BSE, but this time with dynamical effects) produces the kernel[13]

$$K_{n_1 n_2, n_3 n_4}(t) = V_{n_1 n_2, n_3 n_4} \delta(t) - V_{n_4 n_2, n_3 n_1} \delta(t) - \sum_{n_5 n_6, n_7 n_8} V_{n_4 n_2, n_5 n_6} \Pi_{n_5 n_6, n_7 n_8}(-t) V_{n_7 n_8, n_3 n_1}, \quad (15)$$

that in the frequency domain produces the first line from Eq. 22 below.

Upon including higher order terms in the expansion of  $\Pi$ , i.e.,  $\Pi^{(2)} = P^0 K P^0 K P^0$  it can be seen that a ladder series of interactions of this form is present in the reducible polarization  $\Pi(\omega) = P^0(\omega) + P^0(\omega) \tilde{K}(\omega) \Pi(\omega)$ . The kernel for  $n_1 n_2$  and  $n_4 n_3$  particle-hole(hole-particle) pairs (i.e., going beyond the TDA and including the coupling between positive and negative energy transitions; discussed further below) is

$$\tilde{K}_{n_1 n_2, n_3 n_4}(\omega) = \int_0^\infty dt e^{\pm i(\varepsilon_{n_3} - \varepsilon_{n_1})t} K_{n_1 n_2, n_3 n_4}(\mp t) + \int_0^\infty dt e^{\pm i(\varepsilon_{n_2} - \varepsilon_{n_4})t} K_{n_1 n_2, n_3 n_4}(\pm t), \quad (16)$$

where the upper(lower) sign is for  $n_1 n_2$  a particle-hole(hole-particle) pair and  $n_3 n_4$  a hole-particle(particle-hole) pair. The coupling between positive and negative energy transitions can be understood by considering the BSE in the time domain. Even for an instantaneous interaction kernel, the interaction can occur at a time before or after the external particle (or hole) is added, see Fig. 1. Since the interaction is between positive and negative energy propagators (travelling forwards and backwards in time, respectively) and not restricted to the interval where the external particle is present, the interaction is not shifted by the perturbing  $\omega$ . For time-dependent interactions we can also consider the case of  $n_1$  and  $n_2$  both propagating forward or backward in time; considering  $P_{n_1 n_2}^0(1; 3, 4) = -iG_{n_1}(1, 3)G_{n_2}(4, 1)$  for  $t_3 < t_1$  and  $t_4 > t_1$ . These processes describe complex quantum mechanical phenomena such as the emergence of virtual pairs that exist temporarily describing quantum/vacuum fluctuations (as a result of the uncertainty principle) and/or representing intermediate states mediated by the presence of the time-dependent screening. This is beyond the scope of this work, but worth mentioning in the hope of stimulating curiosity.

The functional derivative  $i\delta\Sigma/\delta G$  is discussed in detail in Ref. [13]. From Eq. 14 in that work, the functional derivative can be written as

$$i \frac{\delta\Sigma(3, 4)}{\delta G(5, 6)} = -W(4, 3)\delta(3, 5)\delta(4, 6) - L_{pp}(3, 6; 7, 8)W(6, 3)\chi(7, 4; 5, 8) - L_{ph}(3, 5; 7, 8)W(5, 3)\chi(7, 4; 8, 6), \quad (17)$$

where here it is now assumed that  $\Gamma = 1$  (i.e., the recursive series for  $\Gamma$  is truncated) and  $L$  are two-body correlated propagators that contain correlations between the particles and holes (series of ladder interactions) in the system,

$$\begin{aligned} L_{pp}(1, 2; 3, 4) &= -iG(1, 3)G(2, 4) + \{-iG(1, 5)G(2, 6)\} \times \{-W(6, 5)\} L_{pp}(5, 6; 3, 4) \\ L_{ph}(1, 2; 3, 4) &= -iG(1, 3)G(4, 2) + \{-iG(1, 5)G(6, 2)\} \times \{-W(6, 5)\} L_{ph}(5, 6; 3, 4) \end{aligned} \quad (18)$$

and

$$\chi(7, 4; 5, 8) = W(4, 5)\delta(7, 4)\delta(5, 8) - W(4, 7)\delta(7, 5)\delta(4, 8), \quad (19)$$

that contain a direct and an exchangelike contribution, accounting for exchange between electrons/holes from different electron-hole pairs (arising from the first term on the right hand side of Eq. 17 when considering the recursive series for the vertex). In

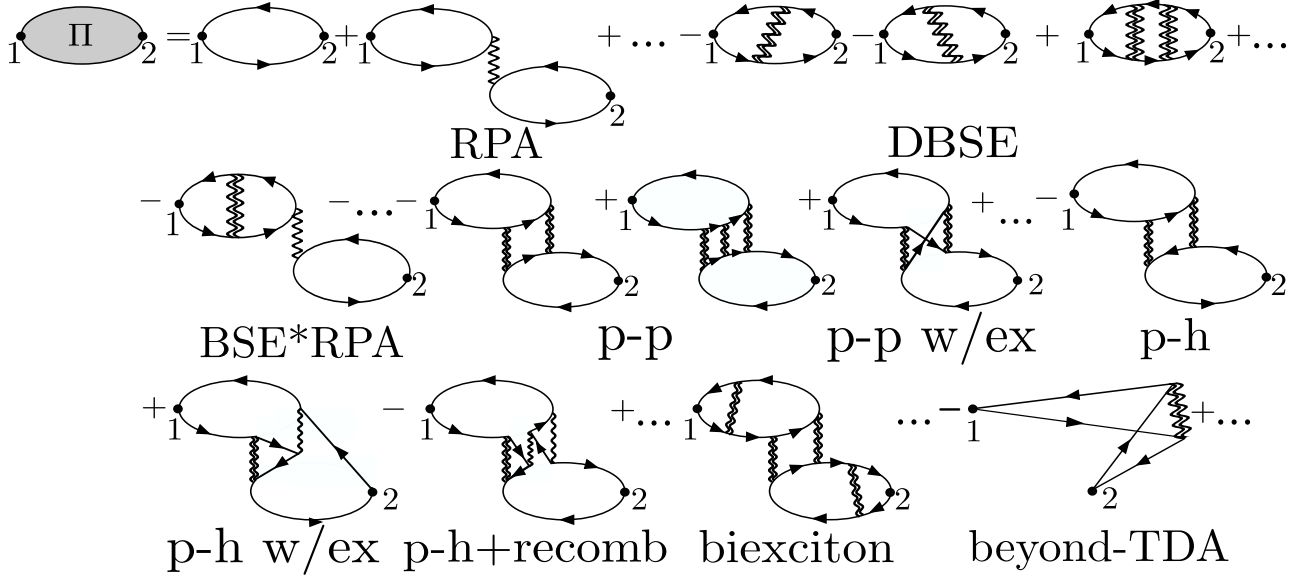


FIG. 1. A subset of the diagrams included in the method for the reducible polarization. The first two terms are part of an infinite series of bubbles that produce the RPA, followed by the infinite ladder series of time-dependent interactions within these bubbles (the dynamical BSE) that excites further electron-hole pairs. Then is the creation of an electron hole pair by the excited particle that arises when considering  $\delta W/\delta G$  in the interaction kernel (with similar diagrams for the hole) and the infinite series of interactions between the electrons and holes with a direct and exchange contribution (from considering  $\delta\Gamma/\delta G$  in the interaction kernel). These channels are coupled, as demonstrated by, e.g., BSE\*RPA, p-p with exchange and the multiexcitonic term. The last term is the coupling diagram for the BSE beyond the TDA (see text). In these diagrams, time can be thought to flow horizontally. Straight lines represent propagators (Green's functions) and single (double) wavy lines represent the bare(screened) Coulomb interaction.

this work, 3-body correlated propagation is suppressed.[13]  $L_{ph}(1, 2; 3, 4)$  is the four-point extension of the usual particle-hole propagator, i.e., the irreducible polarization  $P$ . It was shown in Ref. [13] by including higher order vertices that  $L_{ph}$  can be replaced with the reducible polarization  $\Pi$ , which effectively describes recombination with the creation of new electron-hole pairs, as in the RPA. The reducible polarization is then of the form of the BSE, with kernel

$$K(3, 4; 5, 6) = v(3, 5)\delta(3, 4)\delta(5, 6)\delta(t_3 - t_5) - W(4, 3)\delta(3, 5)\delta(4, 6) - L_{pp}(3, 6; 7, 8)W(6, 3)\chi(7, 4; 5, 8) - \Pi(3, 5; 7, 8)W(5, 3)\tilde{\chi}^{ph}(7, 4; 8, 6), \quad (20)$$

where  $\tilde{\chi}^{ph}$  is the interaction in Eq. 19 but with the exchange interaction replaced with a bare interaction (discussed in Fig. 5 and the surrounding text in Ref. [13]).

The particle-particle and hole-hole, non-correlated propagators  $L(1, 2, 3, 4) = -iG(1, 3)G(2, 4)$  for a single time difference are  $\mp 1/(\omega - (\varepsilon_{n_1} + \varepsilon_{n_2}) \pm i\eta)$  in frequency, or  $ie^{-i(\varepsilon_{n_1} + \varepsilon_{n_2})t}e^{\mp\eta t}\theta(\pm t)$  in time, and the kernel is then

$$K_{\substack{n_1 n_2 \\ n_3 n_4}}(t) = V_{\substack{n_1 n_2 \\ n_3 n_4}}\delta(t) - W_{\substack{n_4 n_2 \\ n_3 n_1}}(-t) - \sum_{\substack{n_5 n_6 \\ n_7 n_8}} L_{\substack{n_5 n_6 \\ n_7 n_8}}(t)\tilde{W}_{\substack{n_4 n_6 \\ n_5 n_1}}\chi_{\substack{n_7 n_2 \\ n_3 n_8}} - \sum_{\substack{n_5 n_6 \\ n_7 n_8}} \Pi_{\substack{n_5 n_6 \\ n_7 n_8}}(t)\tilde{W}_{\substack{n_6 n_3 \\ n_5 n_1}}\tilde{\chi}_{\substack{n_7 n_2 \\ n_8 n_4}}^{ph}, \quad (21)$$

where the  $\tilde{W}$  are assumed static<sup>2</sup> (see Fig. 1). The reducible polarization with this kernel is then represented in Fig. 1 and in the frequency domain the kernel is

<sup>2</sup> These method could be extended to describe time-dependent interactions in the  $T$ -matrix diagrams from Ref. [13].

$$\begin{aligned}
\tilde{K}_{n_3 n_4}^{n_1 n_2}(\omega) = & V_{n_3 n_4}^{n_1 n_2} - V_{n_3 n_1}^{n_4 n_2} \mp \sum_{\lambda, \substack{n_5 n_6 \\ ph}} V_{n_5 n_6}^{n_4 n_2} X_{n_5 n_6, \lambda} \left\{ \frac{X_{\lambda, hp(ph)}^{-1} V_{hp(ph)}^{n_3 n_1}}{\omega + \varepsilon_{n_2} - \varepsilon_{n_3} + E_\lambda \pm i\eta} + \frac{X_{\lambda, ph(hp)}^{-1} V_{ph(hp)}^{n_3 n_1}}{\omega + \varepsilon_{n_4} - \varepsilon_{n_1} - E_\lambda \pm i\eta} \right\} \\
& \mp \sum_{\alpha, \substack{pp'(hh') \\ n_7 n_8}} \left\{ \tilde{W}_{p(h)n_1}^{n_4 p'(h')} \frac{Y_{pp'(hh'), \alpha} Y_{\alpha, n_7 n_8}^{-1}}{\omega + \varepsilon_{n_2} - \varepsilon_{n_3} - \Omega_\alpha \pm i\eta} + \sum_{\alpha, \substack{hh'(pp') \\ n_7 n_8}} \tilde{W}_{h(p)n_1}^{n_4 h'(p')} \frac{Y_{hh'(pp'), \alpha} Y_{\alpha, n_7 n_8}^{-1}}{\omega + \varepsilon_{n_4} - \varepsilon_{n_1} + \Omega_\alpha \pm i\eta} \right\} \chi_{n_3 n_8}^{n_7 n_2} \\
& \pm \sum_{\lambda, \substack{n_5 n_6 \\ ph}} \tilde{W}_{n_5 n_1}^{n_6 n_3} X_{n_5 n_6, \lambda} \left\{ \frac{X_{\lambda, ph(hp)}^{-1} \tilde{\chi}_{p(h)n_2}^{ph}}{h(p)n_4} + \frac{X_{\lambda, hp(ph)}^{-1} \tilde{\chi}_{h(p)n_2}^{ph}}{p(h)n_4} \right\}, \tag{22}
\end{aligned}$$

where the upper(lower) sign is for  $n_1$  a particle and  $Y$  and  $\Omega$  are the eigenvalues and eigenvectors of the particle-particle (hole-hole) matrix, that in the particle-particle basis is  $(\varepsilon_{n_1} + \varepsilon_{n_2})\delta_{n_1 n_3} \delta_{n_2 n_4} \pm W_{n_2 n_4}^{n_3 n_1}$ . Note that for convenience the beyond-TDA

terms have been omitted. Although this equation appears challenging, it is constructed in a similar way to the usual static BSE. The third line is constructed with the same elements as in the first line; and the second line is constructed analogously, instead using the particle-particle(hole-hole) eigenvectors and eigenvalues that can also be used to construct the  $T$ -matrix contributions to the self-energy.[13] As mentioned above, a reduced, mixed particle basis can be used to reduce the memory/storage demands, and the matrix multiplications can be handled with modern accelerated computing techniques. Once the frequency-dependent kernel is constructed the usual BSE for the reducible polarization can be solved by either inversion or diagonalization for the particular frequency. Since the reducible polarization is such that we know the poles of  $W$  exactly, the convolution between  $G$  and  $W$  (to produce the  $GW$  self-energy) can be performed analytically, making use of the Cauchy residue theorem, and so the screening only needs to be calculated with  $\omega$  determined from the poles of  $G$  and the chosen input energy  $\omega$ , that is often set equal to the single particle eigenvalues in many methods, including many QSGW implementations.[18, 22, 23] Note that the indices are composite indices containing wavevector  $\mathbf{k}$  in extended systems and their combinations are dictated by the conservation of momentum.

### III. CONCLUSIONS

An expression for the kernel in the BSE for the reducible polarization was derived from Hedin's equations. The polarization includes a number of 2-body interactions beyond the usual BSE as a result of now including the functional derivative of the screening and vertex in  $i\delta\Sigma/\delta G$ , *ab initio*. A frequency-dependent interaction kernel incorporating RPA, dynamical excitonic and multiexcitonic effects - due to correlations between the particles and holes from different electron-hole pairs - is presented. The terms that couple the positive and negative energy transitions (i.e., going beyond the Tamm-Dancoff approximation) are also considered and found to be independent of frequency and this is discussed along with an intuitive description of the physical processes described by these terms.

The result is the usual 2-body BSE matrix that requires inversion (or diagonalization), but now with a frequency-dependent interaction kernel containing the added diagrams. Since the reducible polarization is calculated instead of the irreducible one, this matrix only needs inverted at a range of known energies (as opposed to requiring the value at a dense range of frequencies required for the numerical frequency convolution to produce the self-energy when using the irreducible one[18]). The reducible polarization also has the benefit that macroscopic quantities such as electron energy loss spectroscopy (EELS),  $1 + v\Pi$ , and optical absorption spectra,  $1/(1 + v\Pi)$ , are readily computed.

As is the case with the BSE, the number of states that can be included will be much less than the total number of possible states in many systems of interest, however, states not included in the method can still be included at a lower level of theory, e.g., RPA, as discussed in Refs [9, 13]. Self-polarization/correlation effects (significant in strongly correlated systems) will be present in the method, however, these are reduced by the competing direct and exchange interactions and can be mitigated by taking steps to ensure states are not included more than once in the expression for the polarization and self-energy (another benefit of making use of the reducible polarization over the irreducible one). The methods can be adopted to consider time-dependent interactions in the  $T$ -matrix diagrams and to also include second-order dynamically screened exchange effects. The method is general and can be incorporated into, for e.g., the quasiparticle self-consistent  $GW$  formalism[9, 18]; that the author has previously extended by incorporating excitonic effects with only the static part of  $W$ [9].

As discussed extensively in Ref. [13], the use of non-interacting Green's functions in many-body theory tends to rely on the Ward identity[18, 48], however, since vertices are now being considered explicitly, interacting Green's functions (as considered

in Ref. [9]) and/or the use of  $Z$ -factors (investigated when examining time-dependent excitonic effects in Ref. [31]) will need to be considered. With the additions discussed above, along with the possibility of including 3-body correlation effects,[39, 49] and the inclusion of spin fluctuations[50] (where  $T$ -matrix channels[51] and the particle-particle correlation function that governs superconductivity[52] are calculated) and phonon effects,[53] a broadly applicable, high-fidelity *ab initio* approach to solving one-, two-, and even three-particle properties of the many-body problem is within reach. The formalism presented will prove beneficial for researchers studying electronic structure theory, nonlinear optics and high-harmonic generation in general systems of interest, including strongly correlated materials.

## ACKNOWLEDGMENTS

The author would like to thank Dermot Green (QUB) for fruitful discussions and all those involved in the *CCP flagship project: Quasiparticle Self-Consistent GW for Next-Generation Electronic Structure*, especially Mark van Schilfgaarde (NREL, Golden, Co.) and Myrta Grüning (QUB).

- 
- [1] P. Hohenberg and W. Kohn, “Inhomogeneous electron gas,” *Phys. Rev.* **136**, B864–B871 (1964).
  - [2] W. Kohn and L. J. Sham, “Self-consistent equations including exchange and correlation effects,” *Phys. Rev.* **140**, A1133–A1138 (1965).
  - [3] A. Seidl, A. Görling, P. Vogl, J. A. Majewski, and M. Levy, “Generalized kohn-sham schemes and the band-gap problem,” *Phys. Rev. B* **53**, 3764–3774 (1996).
  - [4] Vladimir I. Anisimov, Jan Zaanen, and Ole K. Andersen, “Band theory and mott insulators: Hubbard  $u$  instead of stoner  $i$ ,” *Phys. Rev. B* **44**, 943–954 (1991).
  - [5] A. Kutepov, K. Haule, S. Y. Savrasov, and G. Kotliar, “Self-consistent  $gw$  determination of the interaction strength: Application to the iron arsenide superconductors,” *Phys. Rev. B* **82**, 045105 (2010).
  - [6] B Scott Fales and Benjamin G Levine, “Nanoscale multireference quantum chemistry: full configuration interaction on graphical processing units,” *J Chem Theory Comput* **11**, 4708–4716 (2015).
  - [7] Lars Hedin, “New method for calculating the one-particle green’s function with application to the electron-gas problem,” *Phys. Rev.* **139**, A796–A823 (1965).
  - [8] F. Aryasetiawan and O. Gunnarsson, “Electronic Structure of NiO in the GW Approximation,” *Phys. Rev. Lett.* **74**, 3221 (1995).
  - [9] Brian Cunningham, Myrta Grüning, Dimitar Pashov, and Mark van Schilfgaarde, “QSG  $W$ : Quasiparticle self-consistent  $GW$  with ladder diagrams in  $W$ ,” *Phys. Rev. B* **108**, 165104 (2023).
  - [10] Julian Gebhardt and Christian Elsässer, “Dft with corrections for an efficient and accurate description of strong electron correlations in nio,” *Journal of Physics: Condensed Matter* **35**, 205901 (2023).
  - [11] Young-Moo Byun and Jejoong Yoo, “Gpu acceleration of many-body perturbation theory methods in molgw with openacc,” *International Journal of Quantum Chemistry* **124**, e27345 (2024), <https://onlinelibrary.wiley.com/doi/pdf/10.1002/qua.27345>.
  - [12] W. Kohn, “Nobel lecture: Electronic structure of matter—wave functions and density functionals,” *Rev. Mod. Phys.* **71**, 1253–1266 (1999).
  - [13] Brian Cunningham, “Many-body theory beyond  $gw$ : Towards a complete description of two-body correlated propagation,” *Phys. Rev. Res.* **6**, 043277 (2024).
  - [14] Mark S. Hybertsen and Steven G. Louie, “Electron correlation in semiconductors and insulators: Band gaps and quasiparticle energies,” *Phys. Rev. B* **34**, 5390–5413 (1986).
  - [15] F Aryasetiawan and O Gunnarsson, “The  $gw$  method,” *Reports on Progress in Physics* **61**, 237 (1998).
  - [16] Lars Hedin and Stig Lundqvist, “Effects of electron-electron and electron-phonon interactions on the one-electron states of solids,” (Academic Press, 1970) pp. 1–181.
  - [17] S. Di Sabatino, J. Koskelo, J. A. Berger, and P. Romaniello, “Screened extended koopmans’ theorem: Photoemission at weak and strong correlation,” *Phys. Rev. B* **107**, 035111 (2023).
  - [18] Takao Kotani, Mark van Schilfgaarde, and Sergey V. Faleev, “Quasiparticle self-consistent  $gw$  method: A basis for the independent-particle approximation,” *Phys. Rev. B* **76**, 165106 (2007).
  - [19] T. Miyake, F. Aryasetiawan, T. Kotani, M van Schilfgaarde, M. Usuda, and K. Terakura, “Total energy of solids: an exchange- and random-phase approximation correlation study,” *PRB* **66**, 245103 (2002).
  - [20] Abdallah El-Sahili, Francesco Sottile, and Lucia Reining, “Total energy beyond  $gw$ : Exact results and guidelines for approximations,” *Journal of Chemical Theory and Computation* **20**, 1972–1987 (2024), pMID: 38324673, <https://doi.org/10.1021/acs.jctc.3c01200>.
  - [21] Michael P. Surh, Steven G. Louie, and Marvin L. Cohen, “Quasiparticle energies for cubic bn, bp, and bas,” *Phys. Rev. B* **43**, 9126–9132 (1991).
  - [22] Sergey V. Faleev, Mark van Schilfgaarde, and Takao Kotani, “All-electron self-consistent  $gw$  approximation: Application to si, mno, and nio,” *Phys. Rev. Lett.* **93**, 126406 (2004).
  - [23] M. van Schilfgaarde, Takao Kotani, and S. Faleev, “Quasiparticle self-consistent  $gw$  theory,” *Phys. Rev. Lett.* **96**, 226402 (2006).
  - [24] Francesco Sottile, Valerio Olevano, and Lucia Reining, “Parameter-free calculation of response functions in time-dependent density-functional theory,” *Phys. Rev. Lett.* **91**, 056402 (2003).



- [25] Andrea Marini, Rodolfo Del Sole, and Angel Rubio, “Bound excitons in time-dependent density-functional theory: Optical and energy-loss spectra,” *Phys. Rev. Lett.* **91**, 256402 (2003).
- [26] Andrea Marini, Conor Hogan, Myrta Grüning, and Daniele Varsano, “yambo: An ab initio tool for excited state calculations,” *Computer Physics Communications* **180**, 1392 – 1403 (2009).
- [27] C. Franchini, A. Sanna, M. Marsman, and G. Kresse, “Structural, vibrational, and quasiparticle properties of the peierls semiconductor  $\text{Bi}_2\text{Te}_3$ : A hybrid functional and self-consistent GW + vertex-corrections study,” *Phys. Rev. B* **81**, 085213 (2010).
- [28] M. Shishkin, M. Marsman, and G. Kresse, “Accurate quasiparticle spectra from self-consistent gw calculations with vertex corrections,” *Phys. Rev. Lett.* **99**, 246403 (2007).
- [29] Fabien Bruneval, Francesco Sottile, Valerio Olevano, Rodolfo Del Sole, and Lucia Reining, “Many-body perturbation theory using the density-functional concept: Beyond the *gw* approximation,” *Phys. Rev. Lett.* **94**, 186402 (2005).
- [30] Brian Cunningham, Myrta Grüning, Pooya Azarhoosh, Dimitar Pashov, and Mark van Schilfgaarde, “Effect of ladder diagrams on optical absorption spectra in a quasiparticle self-consistent *GW* framework,” *Phys. Rev. Materials* **2**, 034603 (2018).
- [31] Andrea Marini and Rodolfo Del Sole, “Dynamical excitonic effects in metals and semiconductors,” *Phys. Rev. Lett.* **91**, 176402 (2003).
- [32] Jared R. Williams, Nicolas Tancogne-Dejean, and Carsten A. Ullrich, “Time-resolved exciton wave functions from time-dependent density-functional theory,” *Journal of Chemical Theory and Computation* **17**, 1795–1805 (2021).
- [33] Benjamin H. Ellis, Somil Aggarwal, and Arindam Chakraborty, “Development of the multicomponent coupled-cluster theory for investigation of multiexcitonic interactions,” *Journal of Chemical Theory and Computation* **12**, 188–200 (2016).
- [34] Hyun Seok Lee, Min Su Kim, Hyun Kim, and Young Hee Lee, “Identifying multiexcitons in  $\text{MoS}_2$  monolayers at room temperature,” *Phys. Rev. B* **93**, 140409 (2016).
- [35] Victor Chang Lee, Lun Yue, Mette B. Gaarde, Yang-hao Chan, and Diana Y. Qiu, “Many-body enhancement of high-harmonic generation in monolayer  $\text{MoS}_2$ ,” *Nature Communications* **15**, 6228 (2024).
- [36] Andrey L. Kutepov, “Electronic structure of na, k, si, and lif from self-consistent solution of hedin’s equations including vertex corrections,” *Phys. Rev. B* **94**, 155101 (2016).
- [37] Andrey L. Kutepov, “Self-consistent solution of hedin’s equations: Semiconductors and insulators,” *Phys. Rev. B* **95**, 195120 (2017).
- [38] Andrey L. Kutepov, “Full versus quasiparticle self-consistency in vertex-corrected gw approaches,” *Phys. Rev. B* **105**, 045124 (2022).
- [39] Gabriele Riva, Pina Romaniello, and J. Arjan Berger, “Multichannel dyson equation: Coupling many-body green’s functions,” *Phys. Rev. Lett.* **131**, 216401 (2023).
- [40] Carlos Mejuto-Zaera and Vojt ěch Vlěek, “Self-consistency in *gw* $\Gamma$  formalism leading to quasiparticle-quasiparticle couplings,” *Phys. Rev. B* **106**, 165129 (2022).
- [41] Jaroslav Hofierka, Brian Cunningham, Charlie M. Rawlins, Charles H. Patterson, and Dermot G. Green, “Many-body theory of positron binding to polyatomic molecules,” *Nature* **606**, 688–693 (2022).
- [42] C. M. Rawlins, J. Hofierka, B. Cunningham, C. H. Patterson, and D. G. Green, “Many-body theory calculations of positron scattering and annihilation in  $\text{H}_2$ ,  $\text{N}_2$ , and  $\text{CH}_4$ ,” *Phys. Rev. Lett.* **130**, 263001 (2023).
- [43] Giovanni Onida, Lucia Reining, and Angel Rubio, “Electronic excitations: density-functional versus many-body green’s-function approaches,” *Rev. Mod. Phys.* **74**, 601–659 (2002).
- [44] E. E. Salpeter and H. A. Bethe, “A relativistic equation for bound-state problems,” *Phys. Rev.* **84**, 1232–1242 (1951).
- [45] Florian Weigend, Marco Häser, Holger Patzelt, and Reinhart Ahlrichs, “Ri-mp2: optimized auxiliary basis sets and demonstration of efficiency,” *Chemical Physics Letters* **294**, 143–152 (1998).
- [46] Myrta Grüning, Andrea Marini, and Xavier Gonze, “Exciton-plasmon states in nanoscale materials: Breakdown of the tamm-dancoff approximation,” *Nano Letters* **9**, 2820–2824 (2009), pMID: 19637906, <http://dx.doi.org/10.1021/nl803717g>.
- [47] Marcos Casanova-Páez and Lars Goerigk, “Assessing the tamm–dancoff approximation, singlet–singlet, and singlet–triplet excitations with the latest long-range corrected double-hybrid density functionals,” *The Journal of Chemical Physics* **153**, 064106 (2020), [https://pubs.aip.org/aip/jcp/article-pdf/doi/10.1063/5.0018354/15577773/064106\\_1\\_online.pdf](https://pubs.aip.org/aip/jcp/article-pdf/doi/10.1063/5.0018354/15577773/064106_1_online.pdf).
- [48] Riichi Kuwahara and Kaoru Ohno, “Linearized self-consistent gw approach satisfying the ward identity,” *Phys. Rev. A* **90**, 032506 (2014).
- [49] Y. Pavlyukh, E. Perfetto, and G. Stefanucci, “Photoinduced dynamics of organic molecules using nonequilibrium green’s functions with second-born, *gw*, *t*-matrix, and three-particle correlations,” *Phys. Rev. B* **104**, 035124 (2021).
- [50] E. A. Stepanov, V. Harkov, and A. I. Lichtenstein, “Consistent partial bosonization of the extended Hubbard model,” *Phys. Rev. B* **100**, 205115 (2019).
- [51] Dmitrii Nabok, Stefan Blügel, and Christoph Friedrich, “Electron-magnon scattering in ferromagnets from first principles by combining gw and gt self-energies,” *npj computational materials* **7**, 178 (2021).
- [52] Swagata Acharya, Dimitar Pashov, Francois Jamet, and Mark van Schilfgaarde, “Controlling  $T_c$  through Band Structure and Correlation Engineering in Collapsed and Uncollapsed Phases of Iron Arsenides,” *Physical Review Letters* **124**, 237001 (2020).
- [53] Savio Laricchia, Casey Eichstaedt, Dimitar Pashov, and Mark van Schilfgaarde, “Electron-phonon coupling using many-body perturbation theory: Implementation in the questaal electronic structure suite,” (2024), arXiv:2404.02902 [cond-mat.mtrl-sci].